Human Flap Endonuclease-1: Conformational Change upon Binding to the Flap DNA Substrate and Location of the Mg^{2+} Binding Site†

Chang-Yub Kim, Min S. Park,* and R. Brian Dyer

Bioscience Division, Los Alamos National Laboratory, Los Alamos, New Mexico 87545

Received September 6, 2000; Revised Manuscript Received December 22, 2000

ABSTRACT: Human flap endonuclease-1 (FEN-1) is a member of the structure-specific endonuclease family and is a key enzyme in DNA replication and repair. FEN-1 recognizes the 5′-flap DNA structure and cleaves it, a specialized endonuclease function essential for the processing of Okazaki fragments during DNA replication and for the repair of 5′-end single-stranded tails from nicked double-stranded DNA substrates. Magnesium is a cofactor required for nuclease activity. We have used Fourier transform infrared (FTIR) spectroscopy to better understand how Mg^{2+} and flap DNA interact with human FEN-1. FTIR spectroscopy provides three fundamentally new insights into the structural changes induced by the interaction of FEN-1 with substrate DNA and Mg^{2+}. First, FTIR difference spectra in the amide I vibrational band (1600−1700 cm^{-1}) reveal a change in the secondary structure of FEN-1 induced by substrate DNA binding. Quantitative analysis of the FTIR spectra indicates a 4% increase in helicity upon DNA binding or about 14 residues converted from disordered to helical conformations. The observation that the residues are disordered without DNA strongly implicates the flexible loop region. The conversion to helix also suggests a mechanism for locking the flexible loop region around the bound DNA. This is the first direct experimental evidence for a binding mechanism that involves a secondary structural change of the protein. Second, in contrast with DNA binding, no change is observed in the secondary structure of FEN-1 upon Mg^{2+} binding to the wild type or to the noncleaving D181A mutant. Third, the FTIR results provide direct evidence (via the carboxylate ligand band at 1535 cm^{-1}) that not only is D181 a ligand to Mg^{2+} in the human enzyme but Mg^{2+} binding does not occur in the D181A mutant which lacks this ligand.

Flap endonuclease-1 (FEN-1)[1] is known to recognize and cleave 5′-flap DNA, a common structural intermediate that occurs in the processes of DNA replication, recombination, and repair (*1*). In eukaryotic DNA replication, displacement of an upstream primer by an incoming polymerase results in the formation of a 5′-flap structure (*2*, *3*). The 5′-flap intermediates can also be formed during double-stranded break repair (*3*), homologous recombination (*4*), and excision repair (*5*−*8*). For DNA repair and replication, FEN-1's structural recognition of the 5′-flap is essential. The proposed mechanism by which FEN-1 cleaves the 5′-flap is as follows: FEN-1 slides along the 5′ free arm until it reaches duplex DNA (*2*), and at the junction region, it releases the unannealed single-strand region via an endonucleolytic cleavage (*3*, *5*). The molecular details of the DNA recognition, binding, translocation, and cleavage processes, however, are still unknown.

The critical role of FEN-1 in a variety of replication and repair processes, in addition to cleaving 5′-flaps, has been recently recognized. There is evidence that calf FEN-1 functions as a 5′→3′ exonuclease during nick translation (*9*), that SV40 FEN-1 removes the last base of RNA primer attached to Okazaki fragments (*10*), and that *Xenopus laevis* FEN-1 is involved in base excision repair (*8*). In an in vitro replication system of HIV type 1, human FEN-1 was able to cleave the 5′ unannealed tail of the annealed primer, a flap-like structure (*11*). *Saccharomyces cerevisiae* RAD27, a FEN-1 homologue, acts to reduce nonhomologous DNA end-joining (*12*) and plays an active role in preventing trinucleotide repeat expansion and contraction (*13*, *14*). In humans, mutations in FEN-1 may be associated with genetic diseases such as cancer, Huntington's disease, myotonic dystrophy, ataxias, and fragile X syndrome (*15*, *16*). Recently, FEN-1 also has been recognized as an alternative excision repair pathway of UV damage endonuclease (UVDE) for repair of UV photoproducts (*17*). Thus FEN-1 is a crucial enzyme in maintaining genome integrity.

Some structures of enzymes in the same family as human FEN-1 are now known. The structures of *Methanococcus jannaschii* FEN-1 (*Mj* FEN-1) (*18*) and *Pyrococcus furiosus* FEN-1 (*Pf* FEN-1) (*19*) were recently solved, as well as the structure of T4 RNase H (*20*), T5 exonuclease (*21*), and the exonuclease domain of Taq polymerase (*22*), all of which show structural similarity to human FEN-1. All five of these enzymes have identical topology, including in the core region where a β-sheet and associated α-helixes form the base of the active site pocket. This pocket holds the catalytic metal

† This research was supported by the Integrated Structural Biology Resource (LDRD) of Los Alamos National Laboratory.

* To whom correspondence should be addressed. E-mail: park@telomere.lanl.gov. Telephone: (505) 667-5701. Fax: (505) 665-3024.

[1] Abbreviations: DNA, deoxyribonucleic acid; FEN-1, flap endonuclease-1; FTIR, Fourier transform infrared; HIV, human immunodeficiency virus; IR, infrared; *Mj*, *Methanococcus jannaschii*; *Pf*, *Pyrococcus furiosus*; SAXS, small-angle X-ray scattering; TNRs, trinucleotide repeats; Tris-HCl, tris(hydroxymethyl)aminomethane hydrochloride; UVDE, UV damage endonuclease.

10.1021/bi002100n
Published on Web 02/08/2001

ions the enzyme needs to perform its function (*23*). The acidic groups around the metal ion binding sites are generally conserved in this group of enzymes. Of the two metal ion binding sites, one site has been found in almost exactly the same position in each of these five enzymes; the location of the other metal ion binding site varies. Magnesium ions are required by human FEN-1 for the 5′-flap DNA cleavage function.

Through comparison of the amino acid sequences within FEN-1's nuclease family, the conserved amino acids have been identified: Asp34, Asp86, Glu158, Glu160, Asp179, Asp181, and Asp233 (*24*). In human FEN-1, these seven conserved amino acids were found in the active site pocket, all within a 7 Å range around a tightly bound Mg^{2+} ion (*25*).

A flexible loop structure has been identified in *Mj* FEN-1 and *Pf* FEN-1, the two members of the FEN-1 family whose structures are known, as well as in T5 exonuclease (*18*−*21*).

In contrast to the hole-forming structures in topoisomerase (*26*, *27*) and DNA gyrase B protein (*28*), which are able to hold double-stranded DNA, the flexible loop structures in FEN-1 and T5 exonuclease encircle a hole just big enough to accommodate a single-stranded DNA molecule. On the basis of the size of this flexible loop structure and the basic charge distribution on the inside of the loop, it has been proposed that T5 exonuclease, *Mj* FEN-1, and *Pf* FEN-1 may translocate DNA to the cleavage site by a threading mechanism (*18*, *21*). Alternatively, from a study of the effect of flap modification on FEN-1 cleavage, the flexible loop's role was suggested as the thumb subdomain (*29*). In the latter, nuclease tracks along the free 5′-end with a structure which does not fully enclose the flap. The protein structure is open on one side, allowing enough flexibility for the flap to slide past the loop region.

Hosfield et al. determined the crystal structure of the *Pf* FEN-1 protein and postulated that the flexible loop structure changes upon DNA substrate binding on the basis of the flexibility, location near the active site, and size of the loop (*19*). Without a structure of the bound DNA complex, however, this remains to be proven. They also showed that D175 in *Pf* FEN-1, which corresponds to D181 in human FEN-1, is bound to Mg^{2+} and postulated it as a Mg^{2+} ligand in the human enzyme, but again this remains to be demonstrated experimentally.

We have investigated structural changes in human FEN-1 as it binds to Mg^{2+} and to the flap DNA substrate to better understand the mechanism of the enzyme's nuclease activity. In a previous study, we obtained global structural information on human FEN-1 by performing small-angle X-ray scattering. We found no change in human FEN-1 upon its binding to Mg^{2+}, but we found that FEN-1 became more compact upon binding to the flap DNA substrate (*30*).

In the work presented here, we performed Fourier transform infrared (FTIR) spectroscopy to look for conformational changes in human FEN-1 as it binds to Mg^{2+} and as it binds to the flap DNA substrate. FTIR spectroscopy has proven to be a powerful technique for studying the secondary structure of proteins and for tracking structural changes in proteins upon ligand binding (*31*, *32*). The amide I (1600−1700 cm^{-1}) vibrational band arises primarily from the C═O vibration in the peptide backbone. The frequency of the carbonyl stretch is exquisitely sensitive to structural changes in hydrogen bonding and changes in the transition dipole coupling (*33*−*35*). The frequency and intensity of the amide I band have been empirically correlated with secondary structure content (*31*, *32*). Difference FTIR measurements are sensitive to small changes in the structure (i.e., to single chemical bonds) induced by substrate or metal binding to the protein. Finally, the ability to probe the solution structure is particularly important for the analysis of disordered or flexible regions such as FEN-1's flexible loop because crystal packing can induce changes in such structures (*36*, *37*).

We have quantified the secondary structure content of human FEN-1 by deconvolution of the amide I band and find that it is 40% α-helix. Furthermore, when FEN-1 binds to flap DNA substrate, nearly 4% more of its amino acids are converted to α-helical structure, most likely in the flexible loop region. When excess Mg^{2+} is added to FEN-1 (both wild type and the D181A mutant), its secondary structure does not appear to change. The carboxylate vibration band (∼1535 cm^{-1}), however, is sensitive to Mg^{2+} binding to FEN-1. Thus, in addition to providing evidence of changes in secondary structure, FTIR spectroscopic data provide evidence of metal binding.

It is known that Mg^{2+} must be present for FEN-1 to cleave flap DNA and that the seven conserved acidic amino acids interact with two Mg^{2+} ions in the active site pocket (*38*). Mutations of FEN-1 have been produced in which each of the seven conserved amino acids localized near the Mg^{2+} binding sites have been exchanged with alanine. The binding affinity and cleavage activity of each mutant have been reported (*24*, *25*). Out of these seven FEN-1 mutants, only the D181A mutant has shown a binding affinity to flap DNA that is close to that of wild-type FEN-1 (D181A, $K_d = 7.5$ nM; wild type, $K_d = 8$ nM). It appears that the amino acid in the 181 position can be exchanged without affecting the enzyme's binding capability, which suggests that the amino acid in the 181 position is not involved in binding to DNA substrate. Conversely, it appears that the amino acid in position 181 is crucial for cleavage capability. Mutagenesis and kinetics analyses indicate that the Asp181 residue in wild-type FEN-1 is critical in substrate catalysis (*25*). The data we present here show that Asp181 binds to Mg^{2+}, the needed cofactor for cleaving flap DNA.

EXPERIMENTAL PROCEDURES

Protein Purification. The human FEN-1 protein expression and purification were carried out according to the methods of Nolan et al. (*38*). The FEN-1 was eluted from the column poured with TALON Superflow resin (Clontech Laboratories, Inc.) using the elution buffer (20 mM Tris-HCl, pH 7.9, 0.5 M NaCl, and 300 mM histidine). It was further dialyzed in Tris-HCl buffer (pH 7.9) with 100 mM NaCl, 10 mM 2-mercaptoethanol, and 10% glycerol and then concentrated in a Centriprep-10 (Amicon, Inc.) concentrator. Final concentrations were determined by small-angle X-ray scattering (SAXS) using lysozyme as a standard. The purity of the concentrated protein samples was checked by overloaded SDS−polyacrylamide gel electrophoresis (PAGE). The resulting single bands showed ∼99% purity.

Preparation of the 34-mer Flap DNA Substrate. The 5′-flap DNA substrate (34-mer, 5′-CCCCCCATGCTACGTTTT-CGTATACGTTTTCGTA-3′) was synthesized by the solid-

phase phosphoramidite method using an Applied Biosystems synthesizer. We designed a single oligonucleotide which readily forms a 5′-flap structure: it contains two Watson−Crick duplex arms folded by TTTT loops (*39*) and a 10-base-long 5′-flap single strand. This DNA fragment, the substrate, was purified by eluting the material through a POROS R2/H reverse-phase chromatography column, followed, if necessary, by eluting through a POROS HQ/M anion-exchange chromatography column. These procedures were performed in a Bio-Cad Workstation 700E (PerSeptive Biosystems).

The purity of the substrate was analyzed using a TBE-UREA gel (Novex) and found to be more than 98% pure. Nuclear magnetic resonance spectroscopic analysis was used to establish that flaps did indeed form in the DNA substrate. Electrophoretic mobility shift and flap endonuclease assays were used to determine the suitability of the newly designed substrate for FTIR spectroscopic analysis.

Confirmation of Binding and Endonuclease Activity. The binding of both proteins (wild-type FEN-1 and the D181A mutant) to the synthesized substrate was confirmed by gel shift assay, after the 5′-end of the DNA flap substrate was labeled with ^{32}P. The monomeric complex formation between the proteins and flap DNA was confirmed by SAXS *(30)*.

To confirm that our wild-type FEN-1 cleaved the flap DNA substrate and that our D181A mutant did not, we assayed the flap endonuclease activity of the proteins via a flow cytometry-based nuclease assay system (*38*). The presence of Mg^{2+} is required for DNA cleavage, so the proteins were placed in the presence of the flap substrate and Mg^{2+}. Endonuclease activity was also observed with time-resolved SAXS measurements *(30)*.

FTIR Spectroscopic Data and Analysis. Absorption spectra were obtained from (1) wild-type FEN-1 alone, (2) wild-type FEN-1 in the presence of flap DNA substrate, (3) D181A mutant alone, (4) D181A mutant in the presence of Mg^{2+}, and (5) wild-type FEN-1 in the presence of Mg^{2+}. The infrared (IR) spectra were obtained using a Bio-Rad FTS-40 FTIR spectrometer. The protein samples were dialyzed against a D_2O buffer to provide a spectral window in the amide I range. Final FEN-1 protein concentrations used in the FTIR study were ∼2 mg/mL or lower. The protein and flap DNA substrate had a 1:1 stoichiometric molar ratio. The same protein concentrations were applied for both the wild type and the D181A mutant. Mg^{2+} was added in the amount of 10 mM (the molar ratio of Mg^{2+}/protein is ∼210).

The FTIR spectrometer has a dual-compartment cell that holds a 10 μL sample suspended in buffer on one side and the buffer alone on the other side. The sample and reference sides of the cell are identical compartments formed between two 25 mm diameter CaF_2 windows separated by a 50 μm Teflon spacer. Water vapor was purged from the sample cell with N_2 gas, and the data were acquired at 7 °C.

For each sample, both compartments—the sample suspended in buffer and the buffer alone—were scanned 1024 times. An automated shuttle was employed to collect the sample and buffer reference spectra sequentially for each scan, thereby minimizing the effect of instrument drift. The protein absorbance spectrum is computed from the ratio of the single beam spectra of the sample to the reference [$A = -\log(S/R)$]. The final IR absorption spectrum from each sample is the average of the data from the 1024 scans. Difference spectra, as well as the second derivatives of selected spectra, were calculated from the IR absorption spectra. The reproducibility of FTIR data was confirmed by more than four repetitions of each experiment using different preparations of FEN-1 protein and flap DNA substrate for each experiment.

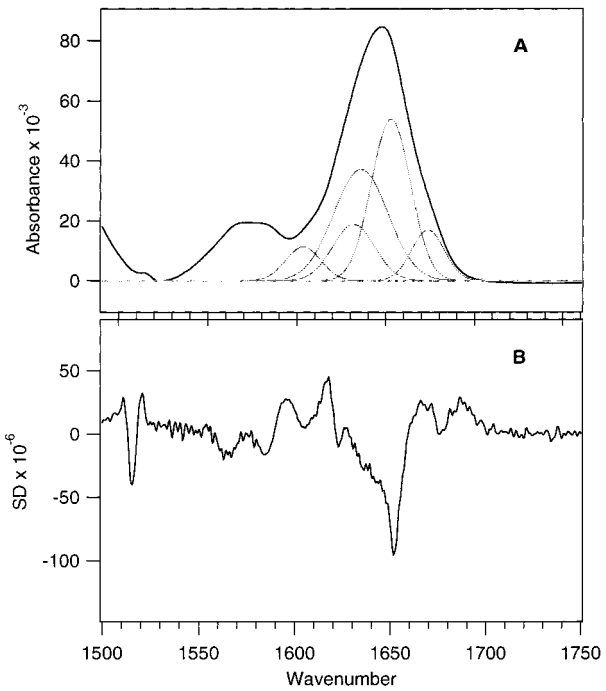

FIGURE 1: Fourier transform infrared (FTIR) absorbance spectrum (A) and the second derivative (B) of wild-type FEN-1 shown in the amide I spectral region. The curves beneath the absorbance spectrum in (A) are the individual Gaussian subcomponents obtained from a spectral deconvolution, as described in the text.

The deconvolution of the amide I band was accomplished using a routine written in Igor (Wavemetrics, Inc.) to perform a Levenberg−Marquardt nonlinear least squares optimization fit to a multi-Gaussian function. The number and positions of the Gaussian subcomponents were determined from the second derivative of the absorbance spectra. Five subcomponents at frequencies determined from the minima of the second derivative in the spectral region between 1600 and 1700 cm^{-1} were defined as the starting parameters of the fit. The intensities and bandwidths were allowed to float in the curve fitting procedure. Allowing the frequencies to float in a second optimization step did not significantly improve the quality of the fit.

RESULTS

Secondary Structure of Wild-Type FEN-1. The correlation of frequencies of amide I subcomponents with specific secondary structures is an area of active research. In some cases, particularly the α-helix, the subcomponent frequencies are well established (*32*, *40*). Our data show that the major absorption spectrum of the wild-type FEN-1 peaks at ∼1650 cm^{-1} (Figure 1A). Absorption in this vibrational band corresponds to α-helical structure.

The second derivative of the absorption spectrum of wild-type FEN-1 in the amide I region (Figure 1B) is dominated by a large minimum at ∼1650 cm^{-1}, confirming that

Table 1: Secondary Structure Content of FEN-1

FTIR (human FEN-1) subcomponent (cm^{-1})/ fraction (%)	assignment	X-ray structure *Pf* FEN-1	X-ray structure *Mj* FEN-1
1632/14	β-sheet	13	13
1640/36	loop/disordered	30	36
1653/40	α-helix	44	44
1674/10	turns	13	7

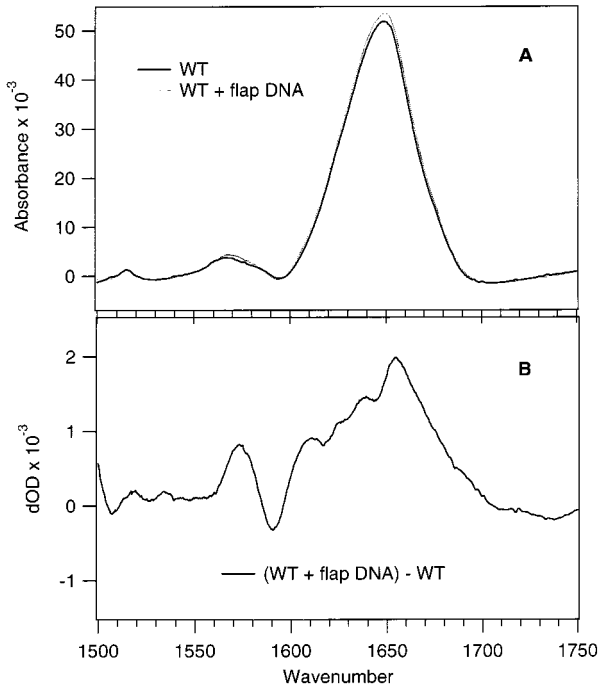

FIGURE 2: FTIR spectra of wild-type FEN-1 in the presence and absence of flap DNA substrate (A) and the difference FTIR spectrum, wild-type FEN-1 with flap DNA minus wild-type FEN-1 alone (B), shown in the amide I spectral region.

α-helical structure is predominant in FEN-1. The second derivative shows several other smaller minima, indicating additional subcomponents in the amide I vibrational band, corresponding to additional secondary structure types. The deconvolution of amide I into subcomponents according to the procedure described above is shown in Figure 1A. The frequencies, relative areas, and assignments of each subcomponent are summarized in Table 1. The assignments are based on empirical correlations previously established for proteins of similar secondary structure content (*32*, *40*). The secondary structure content determined from X-ray crystallography for homologous FEN-1 proteins is also given in Table 1. The agreement is within the error of the deconvolution process, suggesting that the secondary structure content of the human protein is very close to that of the bacterial ones.

Increase in α-Helical Structure upon Binding to Flap DNA. Absorbance of the wild-type FEN-1 sample was ~50 mOD at ~1650 cm^{-1}. When flap DNA substrate was added to FEN-1, the absorbance at ~1650 cm^{-1} rose by ~2 mOD (Figure 2), an increase of about 4% over the original 50 mOD absorbance. This means that approximately 4% of FEN-1's amino acids form new α-helixes. Considering that FEN-1 has 380 amino acids in total, approximately 14 amino acids are involved in the new helical structure. Since ~3.6 amino acids are required to form one helical turn (*41*), we suggest

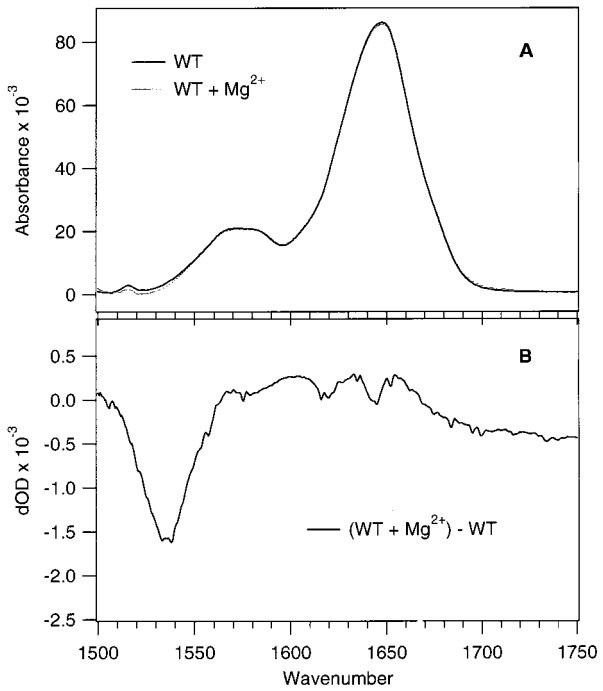

FIGURE 3: FTIR spectra of wild-type FEN-1 in the presence and absence of Mg^{2+} (A) and the difference FTIR spectrum, wild-type FEN-1 with Mg^{2+} minus wild-type FEN-1 alone (B), shown in the amide I spectral region.

that approximately four new helical turns arise when FEN-1 binds to DNA. Furthermore, the broad peak associated with the disordered or loop structure (centered at 1640 cm^{-1}) is decreased in conjunction with the observed increase in the helix peak. Thus, the helix is formed at the expense of the disordered or loop structure upon DNA binding. This observation strongly implicates the flexible loop region of FEN-1 since this is the only stretch of disordered structure (based on the crystal structures of FEN-1 homologues) long enough to account for the observed conversion. Finally, there is a frequency shift in a band (1590 → 1570 cm^{-1}) that we assign to the asymmetric stretch of a carboxylate band that is perturbed upon DNA binding. The exact mechanism for this perturbation is unclear, as it could equally be caused by a change in hydrogen bonding, or metal bonding, or degree of exposure to solvent.

Wild-Type FEN-1 Binding Mg^{2+}. The absorption spectrum of wild-type FEN-1 alone was compared with the absorption spectrum of wild-type FEN-1 in the presence of Mg^{2+} (Figure 3A). Comparison of the two spectra in the amide I vibrational band shows that the structural composition of wild-type FEN-1 is not changed by the addition of Mg^{2+}. At 1650 cm^{-1}, the wavenumber correlated with α-helical structure, there is less than 0.25 mOD difference between FEN-1 alone and FEN-1 in the presence of Mg^{2+}. Relative to FEN-1's absorbance of 80 mOD, this is a change of less than 0.5%.

A distinct change in a carboxylate band of wild-type FEN-1 (~1535 cm^{-1}) was generated by the presence of Mg^{2+} (Figure 3B). The asymmetric stretch of carboxylate occurs in the 1530−1590 cm^{-1} range; the exact frequency depends on the mode of binding (mono- or bidentate) and on the relative strength of hydrogen bonding or metal bonding, with stronger bonding producing a weaker C═O bond and hence a lower C═O frequency. The protonated carboxylic acid group has a single C═O stretch at higher frequency, between

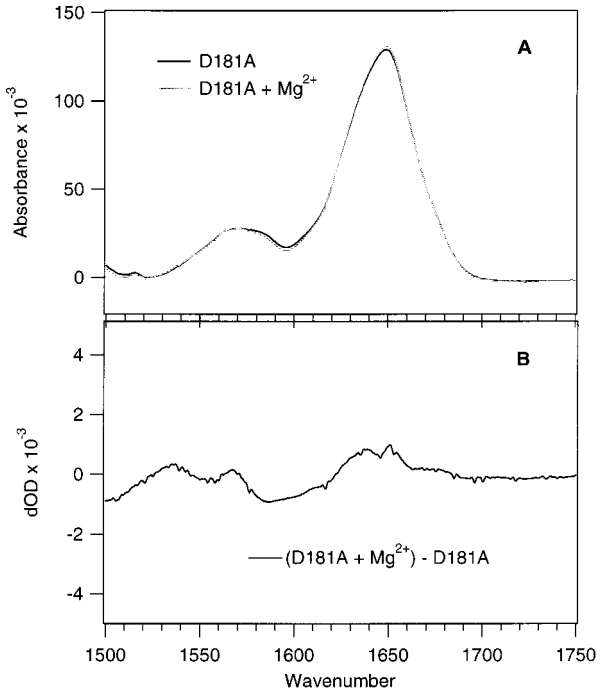

FIGURE 4: FTIR spectra of D181A FEN-1 in the presence and absence of Mg^{2+} (A) and the difference FTIR spectrum, D181A FEN-1 with Mg^{2+} minus D181A alone (B), shown in the amide I spectral region.

1700 and 1760 cm^{-1}. The absence of any peak in the protonated range in the absorbance spectra of FEN-1 with and without Mg^{2+} clearly indicates that all of the carboxylic acid groups are ionized at the experimental pH of 7.9. The spectral change induced by addition of Mg^{2+} is an increase in intensity but not a shift in frequency. These observations are consistent with Mg^{2+} binding to an already ionized carboxylate group or groups, with a concomitant increase in IR intensity. An intensity change without a corresponding frequency shift, together with the unusually low frequency of this band, suggests that this group is strongly hydrogen bonded in the absence of Mg^{2+}, perhaps to water, and that the Mg^{2+} is bound in a bidentate fashion by the carboxylate group.

D181A Mutant. The absorption spectrum of the D181A mutant indicates that the general composition of its secondary structure is the same as that of wild-type FEN-1 (Figure 4A). However, the difference spectra of the D181A mutant alone minus D181A in the presence of Mg^{2+} shows very small (<0.5%) changes (Figure 4B); in particular, the large carboxylate feature in the wild-type difference spectrum is absent for D181A, suggesting that Mg^{2+} does not bind to the latter. Since wild-type FEN-1's spectral changes reveal that it does bind to Mg^{2+} and the only difference between wild-type FEN-1 and the D181A mutant is the amino acid in position 181, it is clear that the wild-type's Asp181 is binding to Mg^{2+}. Therefore, Asp181 can be assigned as one of the amino acids that interact directly with Mg^{2+}.

DISCUSSION

Recent work has highlighted the important role that FEN-1 plays in DNA replication and repair through its function of recognizing and cleaving the 5′-flap DNA structure (*42*, *43*). However, the mechanisms by which FEN-1 recognizes, binds, and cleaves the 5′-flap DNA substrate and the interaction and role of Mg^{2+} within the active site pocket of FEN-1 still have not been well illuminated.

In previous research (*25*, *26*), the seven conserved amino acids (Asp34, Asp86, Glu158, Glu160, Asp179, Asp181, and Asp233) of human FEN-1 were recognized through comparisons with the sequences of other FEN-1 family members (*20*). From the crystal structure of T4 RNase H, which is structurally similar to FEN-1, the position and orientation of each amino acid around the magnesium ions in human FEN-1's active site pocket were proposed (*25*). Recently, the locations of these conserved amino acids around the metal ions were confirmed when the crystal structures of *Mj* FEN-1 (*18*) and *Pf* FEN-1 (*19*) were solved. The locations of the metal ions were also identified.

In the metabolism of DNA polymerases, nucleases, and ligases, magnesium is frequently a required cofactor for the enzymes. This divalent metal is commonly ligated to acidic amino acid residues in the active site of enzymes, where it interacts with water molecules. The resulting nucleophile breaks phosphodiester bonds (*24*). Since the magnesium ions are essential in human FEN-1's reaction with its DNA substrate, it has been hypothesized that the magnesium ions' activation of FEN-1 causes conformational changes that enable FEN-1 to cleave the DNA substrate (*38*). We tested this hypothesis using small-angle X-ray scattering and found no global structural change in human FEN-1 upon the addition of the Mg^{2+} cofactor (*30*).

In the research presented here, we used FTIR spectroscopy to analyze whether any changes in FEN-1's local structure occurred upon binding to Mg^{2+}. Consistent with previous SAXS results (*30*), no reorganization was observed in the secondary structure of either wild-type FEN-1 or the D181A mutant (see 1600−1700 cm^{-1} band in Figures 3 and 4). In addition, the interaction of wild-type FEN-1 with Mg^{2+} turned out to be mediated by Asp181 only, based on the IR absorption spectrum of the D181A mutant which showed that its carboxyl groups were unaffected by the addition of Mg^{2+} (see ∼1535 cm^{-1} band in Figures 3 and 4).

These results suggest that the functions of the two magnesium ions are distinguishable. The one magnesium ion, which seems to be bound tightly in the active site pocket, is not affected by the presence of additional Mg^{2+}. It is likely that the first ion's role is to stabilize the conformation of the overall structure of FEN-1. To keep FEN-1's structure stable, the carboxyl groups of conserved amino acids Asp34, Asp86, Glu158, Glu160, and Asp179 coordinate with the first magnesium ion as ligands on the inside of the active site pocket. The suggested role of this first metal ion is supported by its highly conserved position in *Mj* FEN-1, RNase H, T5 exonuclease, and Tag polymerase enzymes, which have very close structural similarity (*23*).

In contrast, the second magnesium ion is not essential to the structure of FEN-1 and may even be absent in the resting enzyme. FEN-1 binds to the DNA substrate without cutting it in the absence of divalent cations (*2*, *44*), further evidence that only one tightly ligated metal ion is enough for stable protein conformation. It seems that, with the protein structure stabilized by the first metal ion, FEN-1 is capable of binding to the DNA substrate, although it cannot cleave the substrate.

Our FTIR spectroscopic data provide evidence that when wild-type FEN-1 is in the presence of additional Mg^{2+},

Asp181's carboxyl group binds a second magnesium ion. Initially, Asp181 is exposed on the outside of the active site pocket, enabling it to interact with the second magnesium ion and mediate the ion's introduction into the inside of the active site pocket.

We propose two potential roles for the second magnesium ion. The first role is to flag the active site via Asp181 and then guide the DNA into the appropriate configuration for cleavage by the enzyme. The second role is to act as a Lewis acid to activate a nucleophile, which breaks phosphodiester bonds in the substrate cleavage process.

The cleavage reaction requires the presence of FEN-1, Mg^{2+}, and the flap DNA. The mode of the cleavage reaction is not known in detail. It could be that the second magnesium ion binds to Asp181 and then attracts the DNA to the enzyme's active site. Or, since we found in our last study that Mg^{2+} interacts readily with DNA (*30*), the second magnesium ion might initially bind to the DNA. The DNA would then be introduced to FEN-1's active site through the interaction between its magnesium ion and Asp181. Either way, once the proper configuration is in place—a magnesium ion in the middle, bound to Asp181 in FEN-1's active site on one side and bound to the DNA on the other—we postulate that FEN-1 is able to initialize its suggested function of scanning of the DNA substrate, recognizing the 5′-flap structure, and cleaving it.

The study of E160D FEN-1 by Frank et al. (*44*) showed that FEN-1's Glu160 plays a role not only in substrate binding but also in the cleavage process. Probably, its involvement in cleavage happens after Asp181 has bound the DNA in its proper configuration. Turning to our findings about structural change in FEN-1, our FTIR spectroscopic data indicate that FEN-1 forms approximately four new helical turns upon binding to the flap DNA substrate, with a concomitant loss of disordered or loop structure. This secondary structure alteration may occur either due to flap-specific binding or due to nonspecific DNA double strand binding since our binding assay still showed FEN-1's binding activity to double strand DNA (data not shown). This new α-helical structure is most likely formed in FEN-1's flexible loop, both because this is one of the few regions of the protein with a run of disordered or flexible structure sufficiently long enough to accommodate four new turns of α-helix and because, functionally, the new α-helixes would tighten the flexible loop around the DNA substrate it holds (*19*).

Disorder in protein structures such as the flexible loop in FEN-1 has been found locally and globally in numerous X-ray and NMR structures of proteins (*37*, *45*−*49*). In many cases, such unstructured regions of proteins have been linked to biological functions. It is likely that the fast dynamics of such disordered structures allows rapid and specific responses to changing environmental conditions (*50*). Such intrinsic flexibility could allow a single protein to recognize a large number of biological targets without sacrificing specificity, as Bornarth et al. have shown for FEN-1's cleavage activity with variously modified flap substrates (*29*).

The flexible loop region of human FEN-1 likely contains 48 amino acids, based on sequence comparison with *Mj* FEN-1 (*18*). From the charge distribution in this region, the N-terminal side of the flexible loop seems to be a good candidate both for interacting with DNA and for reorganizing into helical structure. We are currently investigating the effects of specific mutations in this loop region on the structure and stability of the DNA complex.

REFERENCES

1. Murante, R. S., Huang, L., Turch, J. J., and Bambara, R. A. (1994) *J. Biol. Chem. 269*, 1191−1196.
2. Murante, R. S., Rust, L., and Bambara, R. A. (1995) *J. Biol. Chem. 270*, 30377−30383.
3. Harrington, J. J., and Lieber, M. R. (1994) *EMBO J. 13*, 1235−1246.
4. Pont, K. G., Dawson, R. J., and Carroll. D. (1993) *EMBO J. 12*, 23−24.
5. Harrington, J. J., and Lieber, M. R. (1994) *Genes Dev. 8*, 1344−1355.
6. Doetsch, P. W. (1995) *Trends Biochem. Sci. 20*, 384−386.
7. Klungland, A., and Lindahl, T. (1997) *EMBO J. 16*, 3341−3348.
8. Kim, K., Biade, S., and Matsumoto, Y. (1998) *J. Biol. Chem. 273*, 8842−8848.
9. Siegal, G., Turchi, J. J., Myers, T. W., and Bambara, R. A. (1992) *Proc. Natl. Acad. Sci. U.S.A. 89*, 9377−9381.
10. Waga, S., Bauer, G., and Stillman, B. (1994) *J. Biol. Chem. 269*, 10923−10934.
11. Rumbaugh, J. A., Fuentes, G. M., and Bambara, R. A. (1998) *J. Biol. Chem. 273*, 28740−28745.
12. Wu, X., Wilson, T. E., and Lieber, M. R. (1999) *Proc. Natl. Acad. Sci. U.S.A. 96*, 1303−1308.
13. Freudenreich, C. H., Kantrow, S. W., and Zakian, V. A. (1998) *Science 279*, 853−856.
14. Schweitzer, J. K., and Livingston, D. M. (1998) *Hum. Mol. Genet. 7*, 69−74.
15. Gordenin, D. A., Kunkel, T. A., and Resnick, M. A. (1997) *Nat. Genet. 16*, 116−118.
16. Tishkoff, D. X., Filosi, N., Gaida, G. M., and Kolodner, R. D. (1997) *Cell 88*, 253−263.
17. Yoon, J.-H., Swiderski, P. M., Kaplan, B. E., Takao, M., Yasui, A., Shen, B., and Pfeifer, G. P. (1999) *Biochemistry 38*, 4809−4817.
18. Hwang, K. Y., Baek, K.-W., Kim, H.-Y., and Cho, Y.-J. (1998) *Nat. Struct. Biol. 5*, 707−713.
19. Hosfield, D. J., Mol, C. D., Shen, B., and Tainer, J. A. (1998) *Cell 95*, 135−146.
20. Mueser, T. C., Nossal, N. G., and Hyde, C. C. (1996) *Cell 85*, 1101−1112.
21. Ceska, T. A., Sayers, J. R., Stier, G., and Suck, D. (1996) *Nature 382*, 90−93.
22. Kim, Y.-S., Eom, S. H., Wang, J.-M., Lee, D.-S., Suh, S. W., and Steltz, T. A. (1995) *Nature 376*, 612−616.
23. Sayers, J. R., and Artymiuk, P. J. (1998) *Nat. Struct. Biol. 5*, 668−670.
24. Shen, B., Nolan, J. P., Sklar, L. A., and Park, M. S. (1996) *J. Biol. Chem. 271*, 9173−9176.
25. Shen, B., Nolan, J. P., Sklar, L. A., and Park, M. S. (1997) *Nucleic Acids Res. 25*, 3332−3338.
26. Lima, C. D., Wang, J. C., and Mondragon, A. (1994) *Nature 367*, 138−146.
27. Berger, J. M., Gamblin, S. J., Harrison, S. C., and Wang, J. C. (1996) *Nature 379*, 225−233.
28. Wigley, D. B., Davies, G. J., Dodson, E. J., Maxwell, A., and Dodson, G. (1991) *Nature 351*, 624−629.
29. Bornarth, C. J., Ranalli, T. A., Henricksen, L. A., Wahl, A. F., and Bambara, R. A. (1999) *Biochemistry 38*, 13347−13354.
30. Kim, C.-Y., Shen, B., Park, M. S., and Olah, G. A. (1999) *J. Biol. Chem. 274*, 1233−1239.
31. Surewicz, W. K., Mantsch, H. H., and Chapman, D. (1993) *Biochemistry 32*, 389−394.
32. Jackson, M., and Mantsch, H. H. (1995) *Crit. Rev. Biochem. Mol. Biol. 30*, 95−120.
33. Krimm, S., and Bandekar, J. (1986) *Adv. Protein Chem. 38*, 181−365.
34. Surewicz, W. K., and Mantsch, H. H. (1988) *Biochim. Biophys. Acta 952*, 115−130.

35. Haris, P. I., and Chapman, D. (1995) *Biopolymers 37*, 251−263.
36. Matter, H., Knauf, M., Schwab, W., and Paulus, E. F. (1998) *J. Am. Chem. Soc. 120*, 11512−11513.
37. Kriwacki, R. W., Hengst, L., Tennant, L., Reed, S. I., and Wright, P. E. (1996) *Proc. Natl Acad. Sci. U.S.A. 93*, 11504−11509.
38. Nolan, J. P., Shen, B., Sklar, L. A., and Park, M. S. (1996) *Biochemistry 35*, 11668−11676.
39. Blommers, M. J. J., Haasnoot, C. A. G., Hilbers, C. W., Van Boom, J. H., and Van der Marel, G. A. (1987) *Struct. Dyn. Biopolym., NATO ASI Ser. E 133*, 78−91.
40. Arrondo, J. L. R., Muga, A., Castresana, J., and Goni, F. M. (1993) *Prog. Biophys. Mol. Biol. 59*, 23−56.
41. Schulz, G. E., and Schirmer, R. H. (1979) in *Principles of Protein Structure* (Cantor, C. R., Ed.) pp 66−107, Springer-Verlag, New York.
42. Lieber, M. R. (1997) *BioEssays 19*, 233−240.
43. Bambara, R. A., Murante, R. S., and Henricksen, L. A. (1997) *J. Biol. Chem. 272*, 4647−4650.
44. Frank, G., Qiu, J., Somsouk, M., Weng, Y., Somsouk, L., Nolan, J. P., and Shen, B. (1998) *J. Biol. Chem. 273*, 33064−33072.
45. van Tilborg, P. J. A., Mulder, F. A. A., De Backer, M. M. E., Nair, M., Van Heerde, E. C., Folkers, G., van der Saag, P. T., Karimi-Nejad, Y., Boelens, R., and Kaptein, R. (1999) *Biochemistry 38*, 1951−1956.
46. Parker, D., Rivera, M., Zor, T., Henrion-Caude, A., Radhakrishnan, I., Kumar, A., Shapiro, L. H., Wright, P. E., Montminy, M., and Brindle, P. K. (1999) *Mol. Cell. Biol. 19*, 5601−5607.
47. Hershey, P. E., McWhirter, S. M., Gross, J. D., Wagner, G., Alber, T., and Sachs, A. B. (1999) *J. Biol. Chem. 274*, 21297−21304.
48. Pavletich, N. P. (1999) *J. Mol. Biol. 287*, 821−828.
49. Fiebig, K. M., Rice, L. M., Pollock, E., and Brunger, A. T. (1999) *Nat. Struct. Biol. 6*, 117−123.
50. Wright, P. E., and Dyson, H. J. (1999) *J. Mol. Biol. 293*, 321−331.

BI002100N